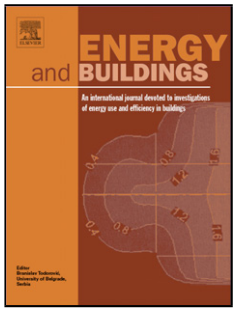

Title: Temperature-induced microstructural changes of fiber-reinforced silica aerogel (FRAB) and rock wool thermal insulation materials: A comparative study

Author: Cristina Siligardi Paola Miselli Elena Francia Magdalena Lassinantti Gualtieri

PII: S0378-7788(16)31805-9
DOI: http://dx.doi.org/doi:10.1016/j.enbuild.2016.12.022
Reference: ENB 7201

To appear in: *ENB*

Received date: 14-6-2016
Revised date: 28-11-2016
Accepted date: 6-12-2016

Please cite this article as: Cristina Siligardi, Paola Miselli, Elena Francia, Magdalena Lassinantti Gualtieri, Temperature-induced microstructural changes of fiber-reinforced silica aerogel (FRAB) and rock wool thermal insulation materials: A comparative study, Energy and Buildings http://dx.doi.org/10.1016/j.enbuild.2016.12.022

Temperature-induced microstructural changes of fiber-reinforced silica aerogel (FRAB) and rock wool thermal insulation materials: A comparative study

*Cristina Siligardi, Paola Miselli, Elena Francia, Magdalena Lassinantti Gualtieri

Department of Engineering "Enzo Ferrari", University of Modena and Reggio Emilia, Via Vivarelli 10/1, 41125, Modena, Italy

Highlights

- FRAB and rock wool display different temperature-induced behavior.
- FRAB devitrifies into carcinogenic cristobalite at high temperature (1400 °C).
- Potential health hazards exists during fire cleanup of FRAB-insulated buildings.
- Being a composite material, FRAB exhibit a two-step sintering behaviour.
- Flammability test results mirror breakdown of organic matter.

Abstract

The strive for improved energy efficiency in the building sector has motivated extended research on high-performance thermal insulation materials, leading to new products available on the market. Fiber-reinforced aerogel is a state-of-the-art material suitable as a substitute for traditional ones such as rock wool, especially for retrofitting and refurbishment of historic buildings where interior insulation may be the only alternative. In view of fire safety, commercial products are already tested and classified according to European standards. However, these tests do not give information on microstructural changes which is important to gain full understanding of the material. Knowledge of the reaction dynamics leading to functional changes of the material is needed in order to take actions to improve product quality. Here, the thermally induced microstructure development of fiber-reinforced silica aerogel blankets and rock wool were investigated using *in-situ* techniques such as thermogravimetry and hot stage microscopy. In addition, X-ray powder diffraction and

Scanning electron microscopy analyses were performed *ex-situ* on thermally treated materials. Flammability was evaluated using cone calorimetry. The results obtained for the two different materials were compared and discussed in view of relationship between microstructure development and fire performance.

Keywords: fiber-reinforced silica aerogel, rock wool, flame retardancy, microstructure

1. Introduction

Buildings account for a major portion of the total energy consumption in the member states of the European Union. Hence, improvement of the energy efficiency in this sector constitutes an important measure to reach the long-term goal dictated in the Kyoto Protocol to substantially reduce greenhouse gas emissions and thus limit the global temperature rise. To this aim, the European parliament and council published "The Energy Performance of Buildings (EPB) directive" 2002/91/EC, revised in 2010 (2010/31/EU), obliging member states to strive for zero-energy buildings. Today in Italy, the legislative decree 63/2013 implements the EPB directives by introducing the Energy Performance Certificate (EPC) which is mandatory for new constructions and sales of buildings.

A promising policy to reach the "zero-energy" goal, is the implementation of Building Energy Regulation Codes (BERC) that are mainly focused on thermal insulation of the envelope [1]. In particular, targets of the overall heat transfer coefficient (U-factor) are dictated thus putting in focus the properties of the insulation materials in use. Recently, Jelle discussed advantages and disadvantages of various thermal building insulation materials [2]. Both traditional ones (e.g. mineral wool, polystyrene-based, cellulose, cork, polyurethane, etc) and state-of-the art ones (e.g. vacuum insulation panels, gas-filled panels, aerogels) were discussed and compared [2]. An important advantage of emerging insulation materials compared to traditional ones is the lower thermal conductivity, allowing to reduce the thickness of building envelopes and thus increase

energy efficiency [2,3]. Reduced insulation thickness is particularly beneficial in the case of retrofitting and refurbishment of historic buildings with facades of cultural value where insulation from the inside may be the only option to decrease the U-factor [4]. The high-performance thermal insulation materials (e.g. aerogel and vacuum insulation panel) allow to minimize inner space loss in these cases [4,5]. This problematic is especially important in countries with a large built heritage like Italy. According to numbers published in 2015 by the Italian National Institute of Statistics (ISTAT), about 25% and 15 % of all Italian residential buildings were built before 1946 and 1919, respectively [6]. Hence, it is not surprising that Italy is the leading country in research on energy efficiency of historic buildings [7].

The most common insulation materials on the Italian market are mineral wools (i.e. glass wool and rock wool). Glass wool is produced from borosilicate glass melt whereas rock wool is obtained from rock melts [2]. Promoted by recent needs to increase the energy efficiency of existing buildings through refurbishment, other materials with higher thermal insulation performance are on the rise. One of these materials, particularly suited for interior insulation, are Fiber-Reinforced Aerogel Blankets (FRAB). Silica aerogels are dried gels having very low weight, high porosity and low density. The materials consist of a cross-linked internal structure of SiO_2 chains with large number of air-filled pores. Pure aerogel has an average pore diameter between 10 and 100nm depending on the purity and the fabrication method, which will take from 85 up to 99.8% of the total aerogel volume [8]. The fiber reinforcement increases the flexibility and compressive strength without compromising the high thermal insulation properties of aerogel [9,10,11].

Regarding building materials in general, it is important to consider reactions that may occur when exposed to fire and possible degradation provoked by these reactions. In view of fire safety, commercial products need to be classified following specific testing procedures indicated in the European standard (EN 13501-1) in order to be CE-marked. Although these tests give indications on the material's thermal behavior from a macroscopic point of view, further experiments are

needed to correlate the observed events with microstructural developments provoked by fire. Such information is important to develop new materials and/or improve existing ones.

In this work, the thermally induced microstructure development of a traditional and an emerging insulating material was investigated. In particular, a direct comparison of thermal behavior was made between rock wool and a FRAB-based insulation material. Results from *in-situ* thermal techniques (i.e. Simultaneous thermogravimetry and differential scanning calorimetry (TG/DSC) and Hot Stage Microscopy (HSM)) was used together with results from *ex-situ* microstructural characterization of heat-treated samples (X-ray Powder Diffraction (XRPD) and Scanning electron microscopy (SEM)). Finally, the flammability was determined for as-received insulation materials using a cone calorimeter (Fire Testing Technology) according to the ISO 5660-1 directives.

The results presented here highlights important differences in microstructural response to heat between rock wool and FRAB, thus contributing to the full understanding of these economically important materials.

2. Experimental procedure

2.1 Materials

Commercial insulation materials based on FRAB and rock wool were studied. The FRAB-based material, having the commercial name Aeropan®, was provided by AMA COMPOSITES, Campogalliano, (MO) Italy. This 10 mm thick sheet material is composed of a flexible FRAB coupled with a rigid membrane of a glass fibers/PP composite.

The rock wool was provided by Rockwool® Italia SpA (Milan, Italy). A mat with a thickness of 60 mm, covered by a polyethylene-coated kraft paper, was investigated. A minor amount of formaldehyde resin and mineral oil is present as binder phase in the rock wool.

2.2. Ex-situ thermal treatments

The effect of temperature on sample microstructure was investigated using samples thermally treated *ex-situ*. The as-received material was fired in an electric kiln for 10 min at a designated temperature without a prior heating step. The firing temperatures were chosen based on *in-situ* characterization techniques as will be discussed later. For the FRAB-based materials, firing was also performed using a heating ramp (10 °C/min up to a maximum temperature of 1400 °C) in order to match the temperature history of samples subjected to the *in-situ* methods (see section 2.4.1).

2.3. Short thermo-hygric treatment

In order to investigate the short-term effect of humidity and moderate temperature on thermal conductivity of the as-received materials, the following experiments were performed: A piece of membrane-supported FRAB (200×200×10 mm) and rock wool mat (200×200×60 mm) were inserted in a climatic chamber (*Climatest* CH 250) set at the following conditions: 48 h at 70±2 °C and 90±5 % relative humidity (RH). The thermal conductivity (see section 2.4.3) was measured before and after aging.

2.4. Characterization methods

2.4.1. In-situ thermal analyses (TGA, HSM)

Thermogravimetric analyses (TGA) were carried out using a NETZSCH STA 409. Samples (ca 100 mg) were loaded in an alumina crucible and heated at a rate of 10 °C/min from 20 to 1400 °C under static air atmosphere. Analyses were performed on representative specimens extracted from the as-received insulation materials (only FRAB in the FRAB-based material).

Hot stage microscopy (HSM, Expert System Solutions) analyses were performed on both the as-received rock wool as well as on the FRAB (detached from the rigid membrane support) using a heating rate of 10°/min up to a maximum temperature of 1600 °C. Samples were prepared as follows: The as-received insulation material was hand-grinded in an agate mortar (ca. 1g). The so-obtained powder was uniaxially pressed into cylinders (length and diameter of 3 mm and 2 mm,

respectively), as this is the only shape that allows to focus on a plane which do not change during the heat-induced transformations. Based on the height (h) and base (b) measured from 2D image recorded *in-situ*, transformation points (sintering, softening, sphere, half-sphere and melting) can be determined by using the MISURA software (v. 3.52) [12]. In addition, sintering curves showing the linear dimensional variation as a function of temperature (i.e. $100 \times h/h_0$) can be drawn.

2.4.2.Chemical and Microstructural characterization (FTIR, XRD, SEM)

Fourier transform Infrared Spectroscopy (FTIR) data for as-received and heat-treated (600 °C) aerogel were collected using a Perking Elmer spectrum 2000 instrument. A fine powder was obtained by collecting the powder segregated from a piece of FRAB following gentle shaking.

The crystalline phases present in the FRAB (detached from the rigid membrane support) and the rock wool before and after thermal treatments were monitored by X-ray diffraction (XRD). These analyses were performed on fine powders obtained by hand-grinding in an agate mortar. The instrument used for data collection was a θ/θ diffractometer (PANalytical, CuKα radiation), equipped with a real time multiple strip (X'Celerator).

In order to study the microstructure and to obtain semi-quantitative chemical analyses of the samples before and after thermal treatment, an environmental scanning electron microscope (ESEM, FEI Quanta 200) equipped with an energy dispersive X-ray spectroscopy system (EDS, Oxford INCA-350) was used. Samples were mounted on aluminum stubs (in-plane view) and gold-coated prior to analyses.

2.4.3.Thermal conductivity

Thermal conductivity (λ) was determined for the as-received insulation materials (membrane-supported FRAB and rock wool mat) before and after the short thermo-hygric treatment previously described in section 2.3. These measurements were performed using a heat flow meter (HFM 436

Lambda 2000, NETZSCH). The test specimen is placed between two parallel plates kept at constant but different temperatures. Thermocouples fixed in the plates measure the temperature drop across the specimen and wireless thermal flux meters (HFMs) embedded in each plate measure the heat flow through the specimen. The thermal conductivity (λ, W/mK) is calculated by means of the heat flux, the temperature difference across the specimen and the thickness of the specimen. Subsequently, the one-dimensional steady state heat flux between the plates (i.e. passing the sample) is determined and the Fourier's law for heat conduction is used to calculate λ.

2.4.4. Functional characterization-flammability tests

Burning properties of as-received insulation materials were investigated using a cone calorimeter (Fire Testing Technology) according to the ISO 5660-1 directives. Two specimens for each thermal insulating materials were tested. Regarding the FRAB-based insulation material, the rigid membrane was removed prior to testing. As for the rock wool sample, the side covered by the kraft paper was facing the heat flux during testing. Cone calorimetry is an increasingly important technique for assessing the fire behavior of materials. Typically, the specimen is irradiated with a heat intensity similar to that experienced in a fire situation (25–75 kW/m^2). In the present work, experiments were performed at a heat flux of 25 kW/m^2, corresponding to a cone temperature of approximately 600 °C. These parameters were selected according to the nature of the material to obtain reasonably ignition rates. A cone shaped heater was used and the specimens had the dimensions 100×100×9 mm^3. The following parameters were determined: time to ignition (TTI), time of flame out (TOF), total heat release (THR) and peak of heat release rate (pHRR).

3. Result and discussion

3.1. General characterization

Fig. 1 shows a cross-sectional sketch view of the as-received FRAB-based insulation material where the SEM micrograph inserts clearly show the morphology of the different layers. The FRAB layer is composed of glass fibers in close association with aerogel particles (white layer in Fig. 1). The rigid support is composed of a glass fiber-reinforced dense amorphous polypropylene (PP) layer (light gray layer in Fig. 1) covered with a thin membrane of PP fibers (dark gray layer in Fig. 1).

Fig. 2 shows low- and high-magnification SEM images of FRAB (a and b, respectively). As can be observed, the fibers are totally covered with pure silica aerogel agglomerates (confirmed by EDS analyses). EDS point analyses on the fibers revealed the presence mainly of Si, Al, Ca and O. Semi-quantitative analyses gave the following approximate weight composition in oxides: SiO_2 64%; CaO 24%; Al_2O_3 10 %; Na_2O+MgO+K_2O+TiO_2+FeO 2%. The chemical composition is only approximate, especially considering that some signal surely comes from the silica aerogel.

Fig. 3 shows the FTIR spectrum collected from the as-received aerogel. For comparison, the spectrum obtained following heating at 600 °C is also shown. The table summary of possible vibrational frequencies and their assignment of surface-modified silica aerogels presented by Al-Oweini and El-Rassy was used for interpretation [13]. The main infrared bands observed at about 1058 cm^{-1} and 790 cm^{-1} in both traces are assigned to vibration modes of silica [13]. The as-received aerogel displays the symmetric C-H stretching and bending vibration (-CH_3 group) at 2963 cm^{-1} and 1251 cm^{-1}, respectively. In addition, the Si-C stretching vibration at 843 cm^{-1} (Si-CH_3) as well as the Si-O in-plane stretching vibrations of the silanol (Si-OH) groups at ca. 940 cm^{-1} are observed [13]. The spectrum is very similar to those obtained by others for hydrophobic silica aerogel modified by trimethyl silylating agents [14,15,16]. This result is not surprising, considering that the material investigated here is destined for use as insulation in buildings. In fact, the replacement of hydrophilic surface Si-OH groups with hydrophobic organic functional groups such as –CH_3 prevents water uptake and thus negative consequences for thermal insulation [17]. Following heating at 600 °C, the peaks assigned to the –CH_3 groups are no longer present in the

spectrum (see Fig. 3). The peak at 940 cm^{-1} assigned to the silanol groups (i.e. Si-OH) is also absent, indicating that heating also results in a dehydroxylation reaction of the silica structure.

Fig. 4 shows low- and high-magnification SEM images of rock wool (a and b, respectively).

The dense fibers show different diameters (range 2-10 microns) and a smooth surface typical of a glassy phase. EDS analyses of the fibers resulted in the following weight composition (main oxides): SiO_2 45 %; CaO 19 %; Al_2O_3 17 %; MgO 10 %; Fe_2O_3 7; Na_2O 2 %. These results are in good agreement with those reported by others for rock wool [18, 19].

The thermal conductivity of the as-received FRAB (membrane-supported) and rock wool were 0.0183 ± 0.0002 $Wm^{-1}K^{-1}$ and 0.0378 ± 0.0002 $Wm^{-1}K^{-1}$, respectively. These values are congruent with expected ones [11]. In order to evaluate the effect of hot and humid environment on thermal conductivity, a high-humidity accelerated aging test was performed (48 h at 70 ± 2 °C and 90 ± 5 % RH) prior to repeated measurements. No change (within errors) was observed in none of the insulation material following aging (0.0187 ± 0.0002 and 0.0374 ± 0.0006 for FRAB-based and rock wool, respectively).

3.2 In-situ thermal analyses-TG/DSC and HSM

Fig. 5a shows the TG/DSC analysis results obtained for the FRAB sample. In the beginning of the heating ramp, adsorbed species are removed (ca. 1.5 wt%) giving rise to an endothermic peak at ca. 60 °C in the DSC curve. Further heating results in at least three exothermic peaks in the DSC curve, with maxima at 250 °C, 515 °C and 680 °C. The first two, rather abrupt, exothermic reactions result in weight losses of about 0.5 wt% and 3 wt.%, respectively (Fig. 5a). The last exothermic event is evidenced by a rather broad peak, associated with a gradual weight loss (ca. 5 wt%) up to a temperature of about 850 °C. As discussed in section 3.1., the FTIR spectra collected from as-received and thermally treated aerogel (600 °C) showed some important differences (Fig. 3). In particular, the spectrum collected from the as-received material displayed peaks associated with $-CH_3$ groups and Si-OH groups that disappeared following thermal treatment at 600 °C. Considering

these data, it is possible to assign the second exothermic event at 515 °C to decomposition of $–CH_3$ groups as found by others [11,16,20]. Instead, the continuous weight loss up to 850 °C is probably due to dehydroxylation (i.e. condensation of silanol groups) also in accordance with earlier work [20,21]. Regarding the first sharp exothermic peak at 250 °C, a clear assignment is difficult although the most probable explanation is decomposition of some organic species not associated directly with the silica structure [20]. Nevertheless, the amount of this compound is very small, considering the low weight loss associated with this peak (ca. 0.5 wt%).

Fig. 5b shows the thermogravimetric analyses results obtained for rock wool. The DSC curve shows three successive exothermic peaks in the range 250-600 °C. These thermal events coincide well with the sole weight loss of ca. 5 wt% observed in the TG trace and is assigned to decomposition of the organic binder present in the insulation material. An additional exotermic event is observed at 920 °C and is assigned to crystallization of the glass fibers. Successive melting of these newly-formed crystals give rise to an endothermic peak at about 1210 °C (see Fig. 5b). In order to identify the formed crystalline phases, XRD data were collected following ex-situ thermal treatment at 900 °C. The results are shown in Fig. 6, together with the pattern collected from as-received rock wool. The as-received glassy material, as indicated by the background hump at 25 °2θ, devitrifies into diopside ($CaMgSi_2O_6$, ICCD file 00-041-1370) and olivine ($Mg_{1.8}$ $Fe_{0.2}SiO_4$, ICCD file 01-079-1197). As already reported in the literature [22,23], these crystalline phases may form during devitrification of glasses belonging to the CaO-MgO-SiO_2 system containing a high amount of Fe_2O_3 as the rock wool studied here (see section 3.2). Fig. 7 shows SEM images of the thermally treated rock wool, showing drastic changes in morphology with respect to the as-received material (compare with Fig. 4). After thermal treatment the fibers are sintered, forming bundles (Fig. 7a). The fiber surface is completely recrystallized (Fig. 7a). Many fibers are hollow due to the devitrification process, see Fig. 7b. These results are in concert with the observations of heat-treated rock wool found elsewhere [19].

HSM is a fast and simple procedure that directly visualizes the thermal modification of a samples during a controlled heating cycle. In particular, the sintering temperature (i.e. temperature at which particles are welded together, thus reaching maximum contraction), the softening temperature and the melting temperature can be evidenced. Fig. 8a and b show the sintering curves (sample height as a function of temperature) for FRAB and rock wool, respectively. Regarding FRAB, it should be reminded here that the material under investigation is a composite (i.e. aerogel+fibre-reinforcement) wherefore the observed trends mirror the overall behavior of the materials mix.

As can be observed in Fig. 8a, the FRAB remains in an expanded (ca. 4 %) state up to a temperature of about 485 °C. This is explained by thermal expansion and possibly also by fast development of gaseous species (evaporation of adsorbed molecules and by decomposition of organic species, see TG/DSC data in Fig. 5a) that contributes to the expansion of the pressed powder. Further heating above 485 °C results in continuous contraction of the compact up to a temperature of ca. 990 °C. Dimensional stability is observed up to about 1150 °C after which further contraction is followed by softening (1340 °C) and melting (1440 °C). The presence of two separate contraction steps possibly mirrors different sintering points for the fibre-reinforcement and the silica aerogel.

Woignier et al. studied the sintering behaviour of silica aerogel and found that sintering due to a diffusional process occurs in the temperature range 500-700 °C whereas viscous sintering prevails above 1000 °C [20]. Considering the results reported by Woigner, the first contractions step (identified sintering temperature of 887 °C, see Fig. 8a) is possibly related to sintering of aerogel. The second large contraction above 1150 °C is possibly a combined effect from sintering of both the fiber-reinforcement as well as the silica aerogel particles. In order to verify these assumption, SEM images were collected of samples treated *ex-situ* at 800 °C and 1400 °C. The results are presented in Fig. 9 a and b, respectively. In accordance with the conclusions drawn from the sintering curves depicted in Fig. 8a, heating at 800 °C apparently results in sintering of the silica aerogel clusters leaving the glass fibers totally uncovered (see Fig. 9a) and apparently unchanged. Further heating at 1400 °C leads to a highly sintered and partly melted material. Some fiber relicts

are present, as indicated by arrow in Fig. 9b. It is interesting to observe that the surface is partly covered with small crystals. In order to identify their nature XRD patterns were collected from thermally treated FRAB (10°C/min up to 1400 °C) and the results are shown in Fig. 10. For comparison, the XRD pattern collected from the as-received material is also shown. The amorphous nature of the as-received FRAB material is not conserved following heating at 1400 °C (see Fig. 10). The material devitrifies, thus forming cristobalite as expected (Fig. 10). Evidence of devitrification was however not observed in the DSC curve of FRAB (see Fig. 5a), probably due to sluggish reaction. Considering that cristobalite is classified as carcinogenic, worker safety during fire cleanup and subsequent safe disposal are important considerations [19].

Fig. 8b shows the sintering curve recorded for rock wool. An initial expansion behaviour is observed in the temperature range 390-470 °C, followed by a contraction in the range 730-820 °C. According to the TG results (Fig. 5b), the organic binder (formaldehyde resin/mineral oil) starts to decompose at around 400 °C which corresponds well with the temperature range in which expansion was observed. Hence, gaseous products evolved by these reactions possibly contributed to the trend observed in the sintering curve.

At a temperature of 1154 °C the sintering point is reached, whereas softening and melting is observed at 1186 °C and 1223 °C, respectively. These characteristic temperatures are almost identical with the ones found by Gualtieri et al. for a commercial rock wool [19].

3.3 Flammability tests

Following 11 s after the beginning of the flammability test, the FRAB material was ignited (i.e. time to ignition, TTI). Quite low flames, similar to glowing ember, were homogeneously distributed over the surface as can be observed in Fig. 11. The material continued to glow for about 1 min (time of flame out, TOF). A peak of heat release rate (pHRR) of 45 kW/m^2 was observed after approximately 20 s. The total heat released (THR) was about 3.6 MJ/m^2. The development of fumes

was very low, almost impossible to observe with the naked eye. Considering that the cone temperature is approximate 600 °C (see section 2.4.4.), this visible surface effect is probably related to the decomposition of the methyl groups on the internal surface of the aerogel particles as found by others [24]. In fact, the TG/DSC results combined with the FTIR study showed that a temperature of 600 °C is high enough to obtain complete decomposition of these functional groups (see Fig. 5a and related discussions).

The polyethylene-coated kraft paper covering the rock wool showed withdrawal and partial melting after about 9 s from the opening of the cone (not shown here). In addition, a bulge was formed by the expansion of this layer. After about 20 s, the material was ignited (TTI) and combustion lasted for about 4 min (i.e. TOF), leading to a total heat release (THR) of 23 MJ / m^2. The peak heat release rate (pHRR) occurred after 35 s, being ca. 169 kW/m^2.

The time required to ignite the samples is quite low for both materials (19 s for rock wool and 11 s for FRAB), whereas the flame extinguishing time is considerably greater for rock wool (4 min) compared to FRAB (1 min). The other measured parameters associated with the burning properties were all higher for the rock wool insulation material. This was of course expected, considering the burning potential of the kraft paper covering the exposed side of the insulation material.

4. Conclusions

In this work, the thermally induced microstructure development of rock wool and fiber-reinforced aerogel blankets (FRAB) were investigated in view of response to real fire.

According the TG/DSC data in combination with ex-situ FTIR analyses, the FRAB material looses about 8 wt% during heating up to about 850 °C due to decomposition of surface hydrophobizer (i.e. methyl groups) and dehydroxylation of silanol groups. The TG/DSC curves of rock wool show complete decomposition of the organic binder phase at 600 °C, leading to a total weight loss of 5 wt.%. Devitrification of the glassy fibers were observed at 920 °C. The newly-formed crystalline phases were identified as diopside and olivine by XRD.

The sintering curve of FRAB determined by hot stage microscopy (HSM) showed two separate contraction steps (ca 500-990 °C and >1150 °C), most probably mirroring different sintering points for the fibre-reinforcement and the silica aerogel. The melting point of the FRAB is considerably higher that the one for rock wool (1440 °C versus 1223 °C). According to SEM and XRD analyses of heat-treated FRAB, crystallization of cristobalite occurs following prolonged heating at 1400 °C. Some safety concerns regarding fire cleanup and subsequent handling and disposal of waste material is thus raised, considering that cristobalite is classified as carcinogenic.

Results from flammability tests by cone calorimetry mirrored the decomposition of organic species present in the different materials. According to these tests, the FRAB was more fire resistant compared to the rock wool panel. Time of extinction of the flame in FRAB was found to be four times inferior than the corresponding value obtained for the rock wool panel. In addition, the total heat release was smaller (3 MJ / m^2 compared to 23 MJ / m^2 for rock wool). These results were explained by the kraft paper covering the rock wool panel, thus reducing the fire resistance.

Acknowledgements

The authors would like to thank Marco Corradini e Alberto Donelli, AMA COMPOSITES (Campogalliano, Modena, Italy) for providing the FRAB-based insulation boards.

References

[1] G. Salvalai, G. Masera, M.M. Sesana, Italian local codes for energy efficiency of buildings: Theoretical definitions and experimental application to a residential case study, Renewable and Sustainable Energy Reviews, 42 (2015) 1245-1259

[2] B.P. Jelle, Traditional, state-of-the-art and future thermal building insulation materials and solutions-Properties, requirements and possibilities, Energy and Buildings 43 (2011) 2549-2563.

[3] E. Cuce, P.M. Cuce, C.J. Wood, S.B. Riffat, Optimizing insulation thickness and analyzing environmental impacts of aerogel-based thermal superinsulation in buildings, Energy and Buildings, 77 (2014) 28-39.

[4] J. Zagorskas, E.K. Zavadskas, Z. Turskis, M. Burinskiene, A. Blumberga, D. Blumberga, Thermal insulation alternatives of historic brick buildings in Baltic sea region, Energy and Buildings 78 (2014) 35-42

[5] K. Ghazi Wakili, B. Binder, M. Zimmerman, C. Tanner, Efficiency verification of a combination of high performance and conventional insulation layers in retrofitting a 130-year old building, Energy and Buildings 82 (2014) 237-242.

[6] Costruzioni, in: Annuario Statistico Italiano, ISTAT, 2015, pp. 581-601

[7] A. Martínez-Molina, I. Tort-Ausina, S. Cho, S.-L. Vivancos, Energy efficiency and thermal comfort in historic buildings: A review, Renewable and Sustainable Energy Reviews 61 (2016) 70–85

[8] M.J. van Bommel, C.W. den Engelsen, J.C. van Miltenburg “A thermoporometry study of fumed silica/aerogel composites” Journal of Porous materials 4 (1997) 143-150

[9] X. Yang, Y. Sun, D. Shi, J. Liu, Experimental investigation on mechanical properties of a fiber-reinforced silica aerogel composite, Materials Science and Engineering A A 528 (2011) 4830-4836

[10] R.Baetens, B.P. Jelle, A. Gustavsen, Aerogel insulation for building applications: A state-of-the-art review, Energy and Buildings 43 (2011) 761-769.

[11] E. Cuce, P.M: Cuce, C.J. Wood, S: B. Riffat “Toward aerogel based thermal superinsulation in buildings: A comprehensive review Renewable and sustainable energy reviews, 34 (2014) 273-299

[12] D. Sighinolfi, Misura® equipment, solving ceramic problems, Ind Ceram 30 (2010) 1-8

[13] R. Al-Oweini, H. El-Rassy, Synthesis and characterization by FTIR spectroscopy of silica aerogels prepared using several Si(OR)4 and R"Si(OR')3 precursors, Journal of Molecular Structure 919 (2009) 140-145.

[14] D. Ge, L. Yang, Y. Li, J. Zhao, Hydrophobic and thermal insulation properties of silica aerogel/epoxy composite, J Non-crystalline solids 355 (2009) 2610-2615.

[15] P.M. Shewale, A.V. Rao, A.P. Rao, Effect of different trimethyl silylating agents on the hydrophobic and physical properties of silica aerogels, Appl Surf Sci 254 (2008) 6902-6907

[16] A.V. Rao, M.M. Kulkarni, D.P. Amalnerkar, T. Seth, Superhydrophobic silica aerogels based on methyltrimethoxysilane precursor, J Non-crystalline solids 330 (2003) 187-195

[17] A. S. Dorcheh, M.H. Abbasi, Silica aerogel; synthesis, properties and characterization, Journal of materials processing technology 199 (2008) 10-26

[18] K. Luoto, M. Holopainen, J. Kangas, P. Kalliokoski, K. Savolainen, Dissolution of Short and Long Rockwool and Glasswool Fibers by Macrophages in Flow through Cell Culture, Environ Res. 78 (1998) 25-37.

[19] A.F. Gualtieri, E. Foresti, I.G. Lesci, N. Roveri, M. Lassinantti Gualtieri, M. Dondi, M. Zapparoli, Journal of Hazardous Materials, 162 (2009) 1494-1506

[20] T. Woignier, J. Phalippou, M. Prassas, Glasses from aerogels Part 2 The aerogel-glass transformation, Journal of Materials science 25 (1990) 3118-3126.

[21] J Matyáš, M.J. Robinson, G.E. Fryxell, The effect of temperature and uniaxial pressure on the densification behaviour of silica aerogel granules. In: Ceramic Materials for energy applications II, Ceramic Engineering and Science Proceedings, Vol. 33., issue 9, 2012. Ed. K. Fox, Y. Katoh, H.-T. Lin, I. Belharouak pp. 121-132.

[22] A.M. Marabini, P. Plescia, D. Maccari, F. Burragato, M. Pelino, New materials from industrial and mining wastes: glass-ceramics and glass- and rock-wool fibre, Int. J. Miner. Process. 53 (1998) 121-134.

[23] G.A. Khater, A. Abdel-Motelib, A.W. El Manawi, M.O. Abu Safiah "Glass-ceramics materials from basaltic rocks and some industrial waste, J. Non-Crystalline Solids 358 (2012) 1128–1134.

[24] K. Ghazi Wakili, A. Remhof, Reaction of aerogel containing ceramic fibre insulation to fire exposure, Fire Mater (2016).

Figure captions

Fig. 1: Cross-sectional sketch view of the FRAB-based insulation material, including SEM micrographs showing the in-plane layer morphology (see text for details).

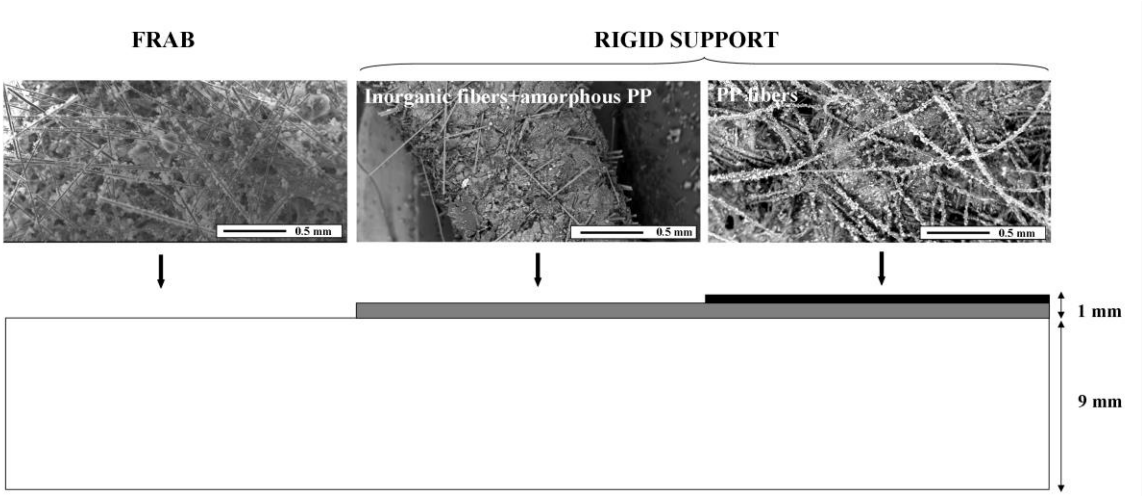

Fig. 2: Low- and high-magnification SEM images of FRAB (a and b, respectively).

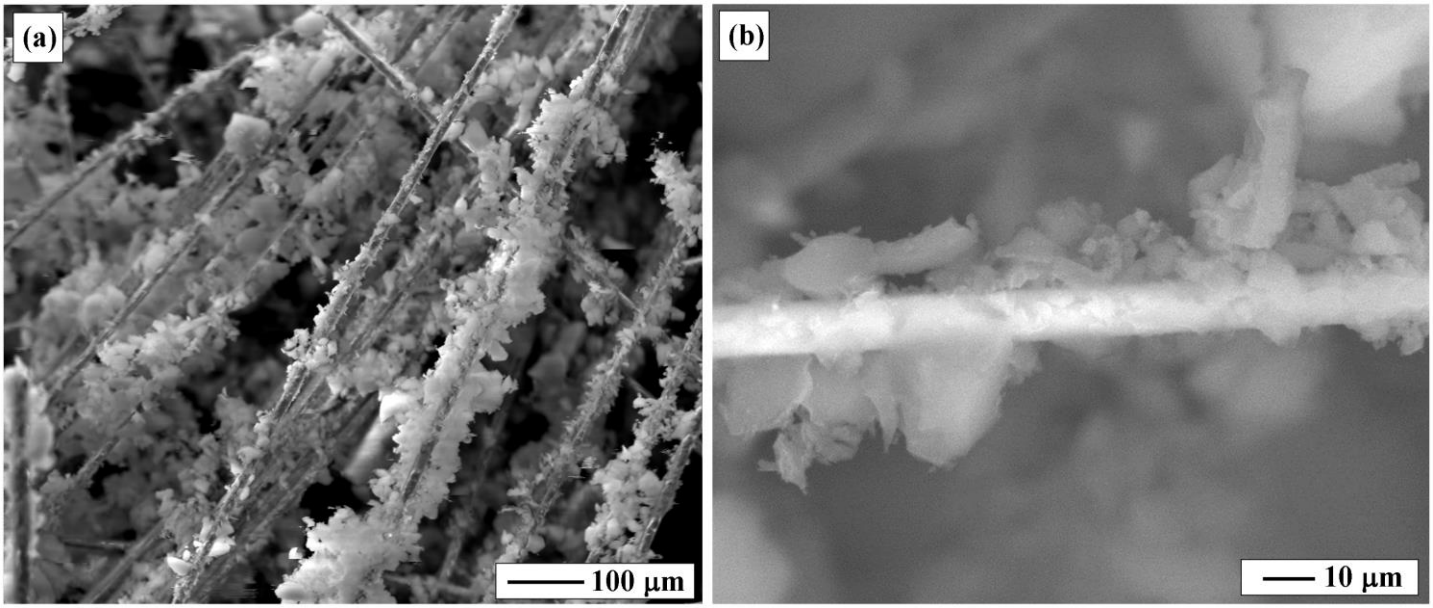

Fig. 3: FTIR spectra collected from the aerogel before and after heating at 600 °C.

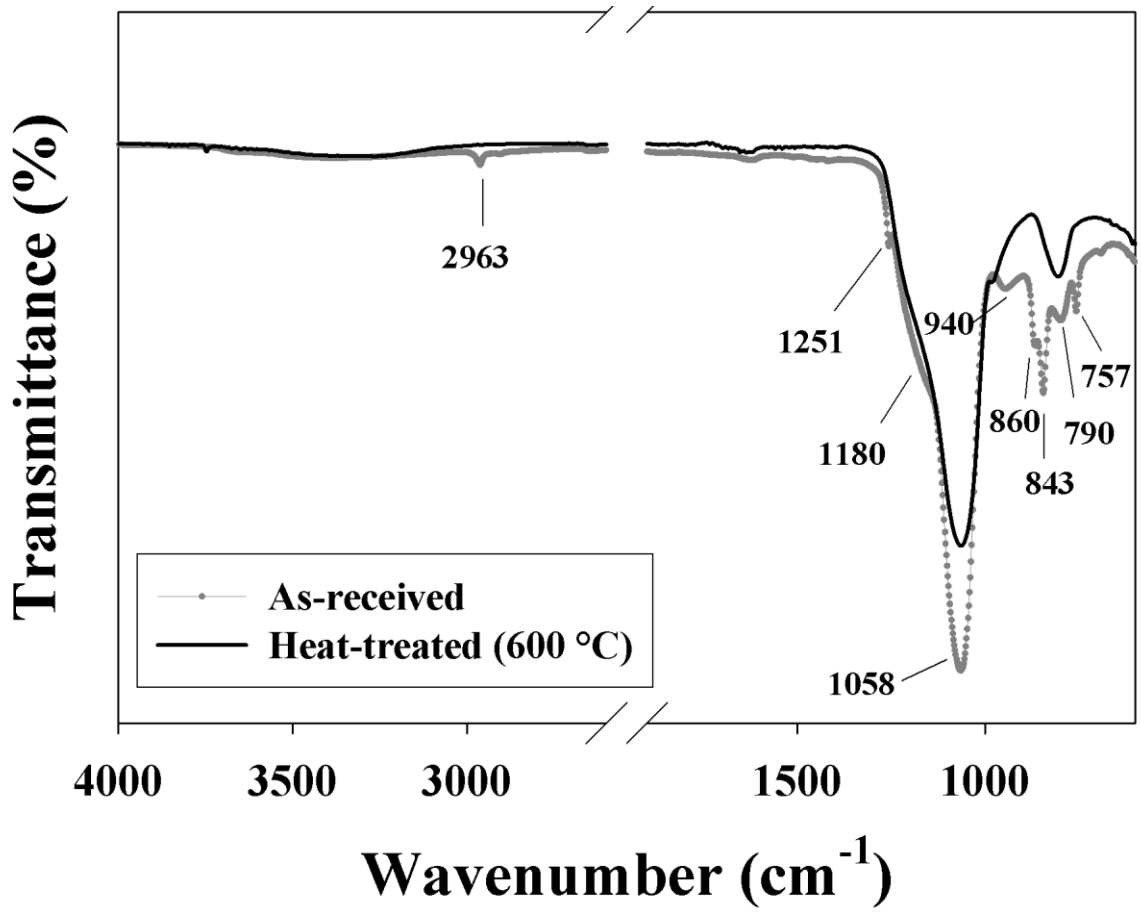

Fig. 4: Low- and high-magnification SEM images of rock wool (a and b, respectively).

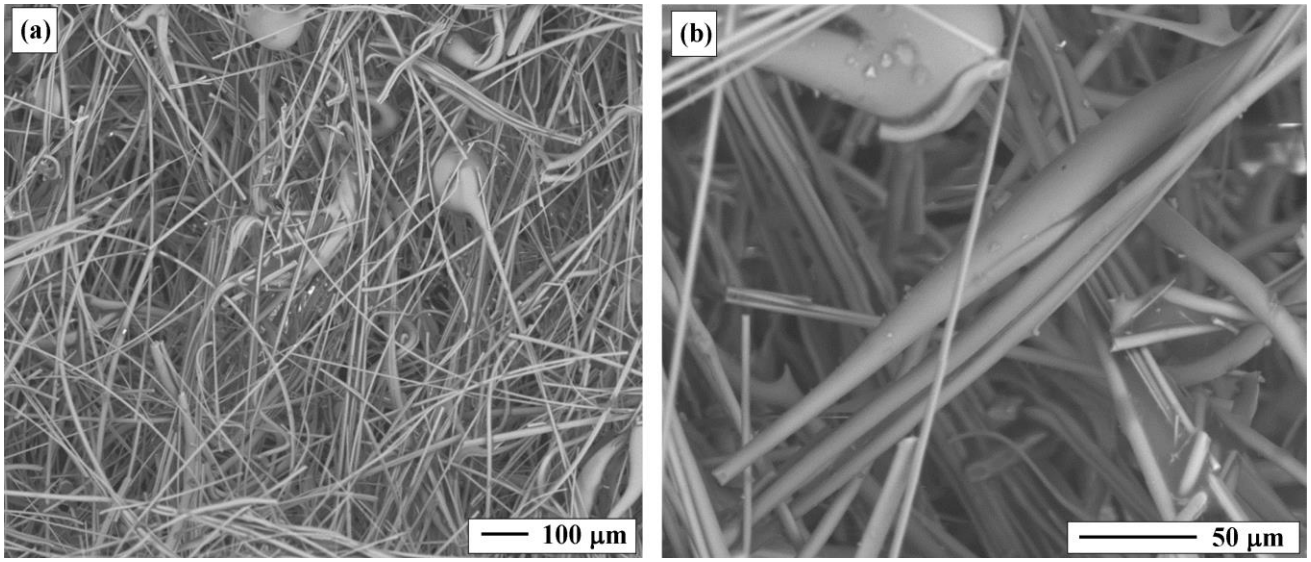

Fig. 5a: TG/DSC analysis results obtained for the FRAB.

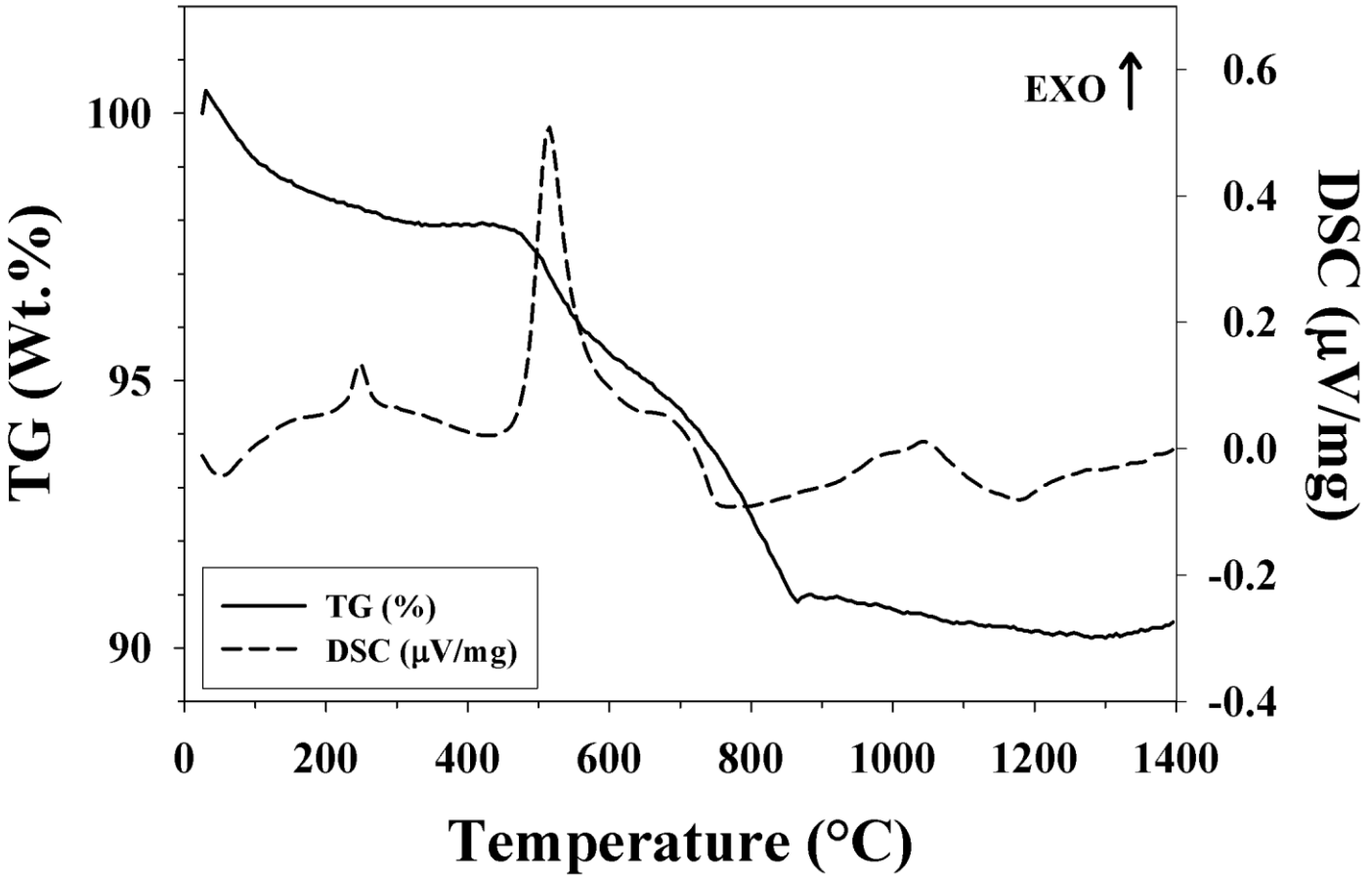

Fig. 5b: TG/DSC analysis results obtained for the rock wool.

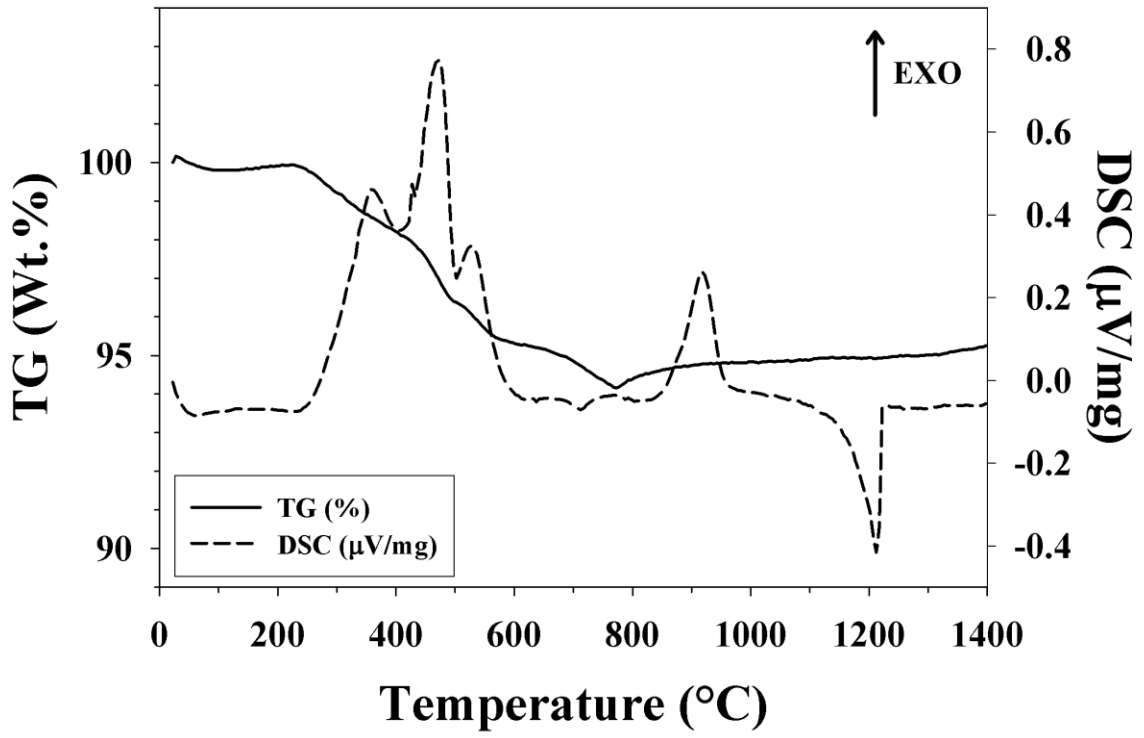

Fig. 6: XRD analyses results obtained for as-received and heat-treated (900 °C) rock wool.

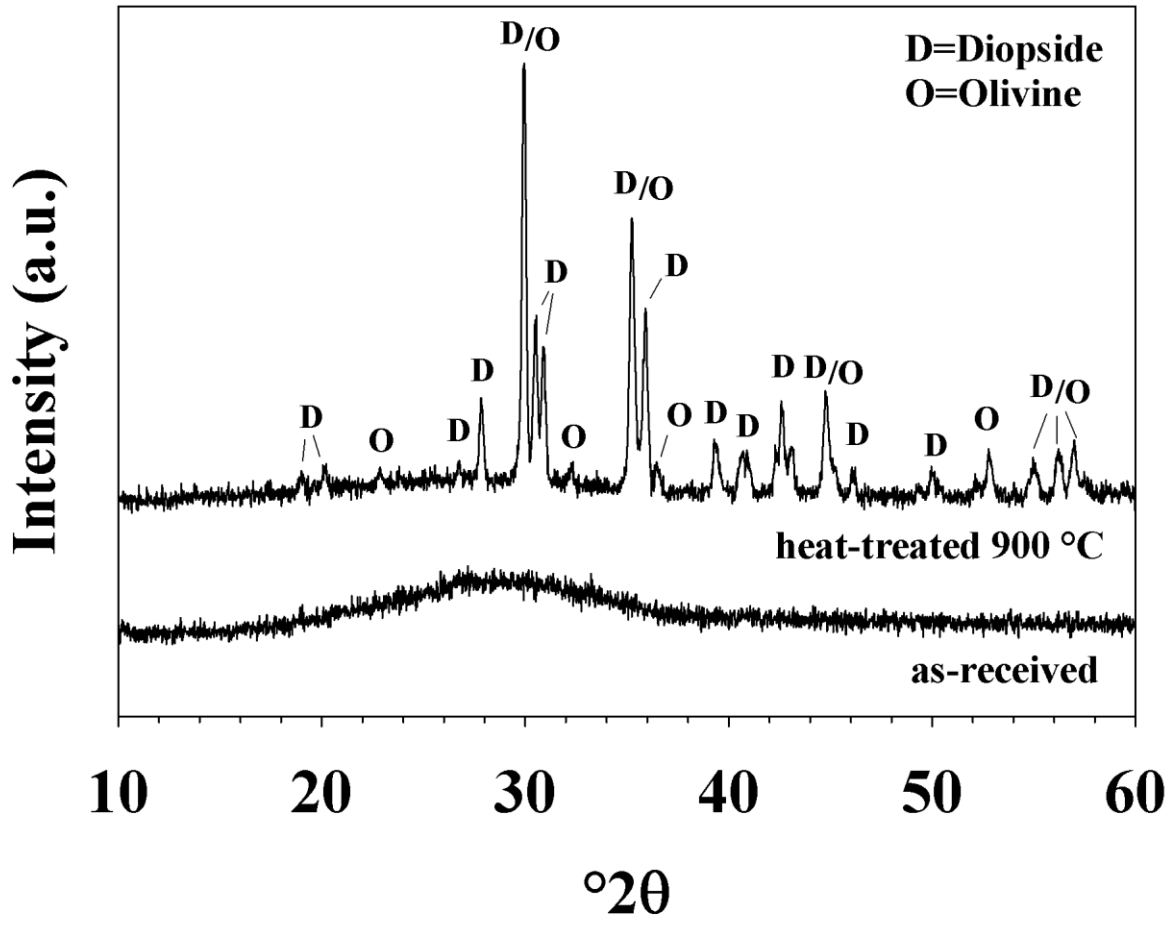

Fig. 7: SEM images of rock wool thermally treated at 900 °C, showing bundles (a) and fibercavities (b) due to sintering and recrystallization.

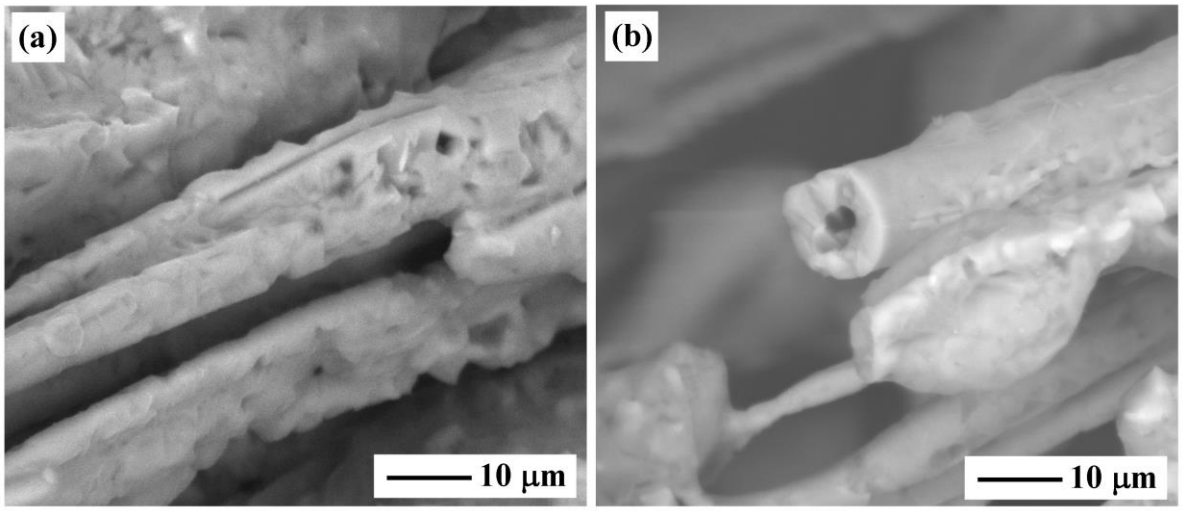

Fig. 8: Sintering curves (sample height as a function of temperature) as determined using hot stage microscopy (HSM) for FRAB (a) and rock wool (b). The vertical lines indicate the characteristic temperatures (i.e. sintering, softening, melting).

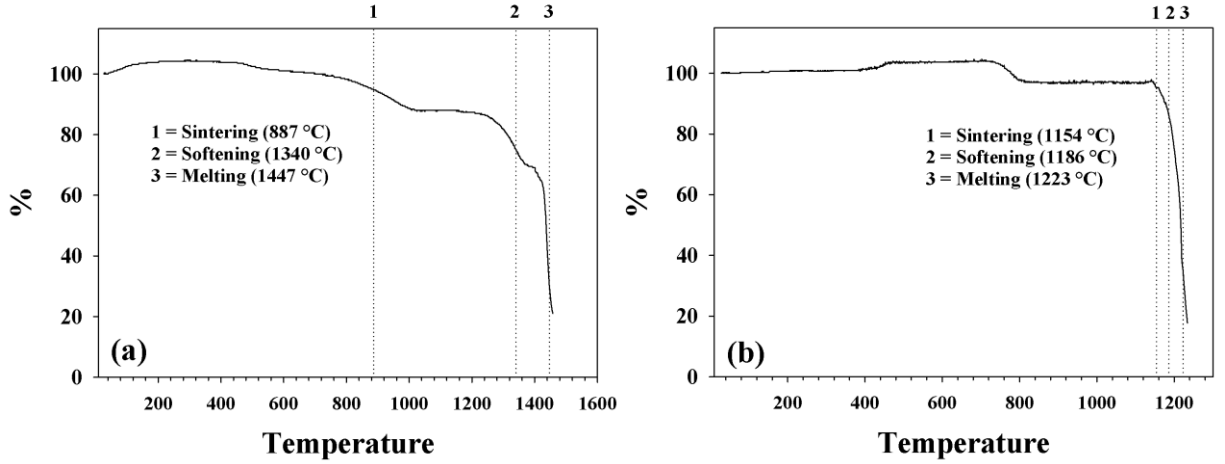

Fig. 9: SEM images of FRAB heat-treated at 800 °C (a) and 1400 °C (b). The insert in (b) highlights the newly-formed crystals observed on the partially melted material.

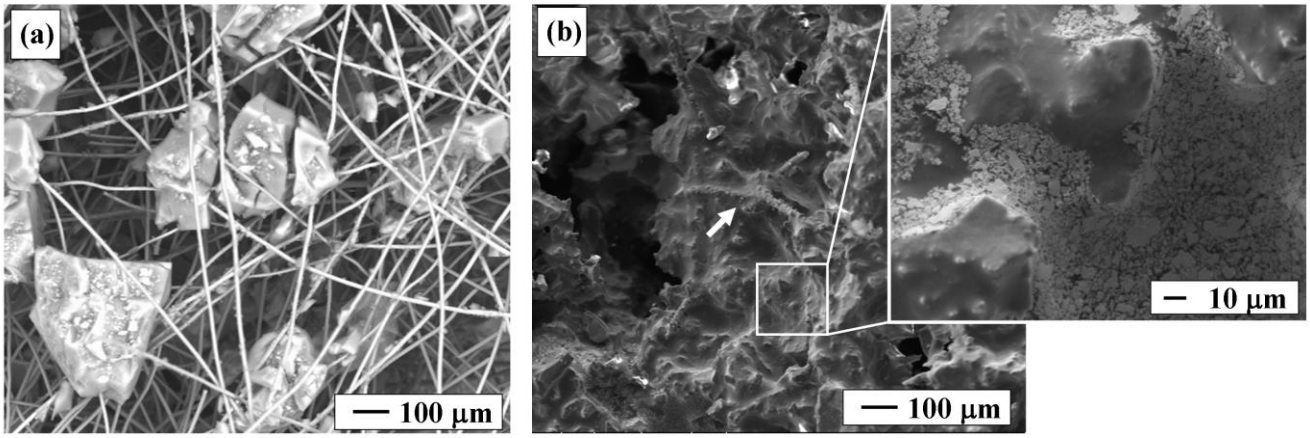

Fig. 10: XRD patterns collected from as-received and thermally treated FRAB (10°C/min up to 1400 °C).

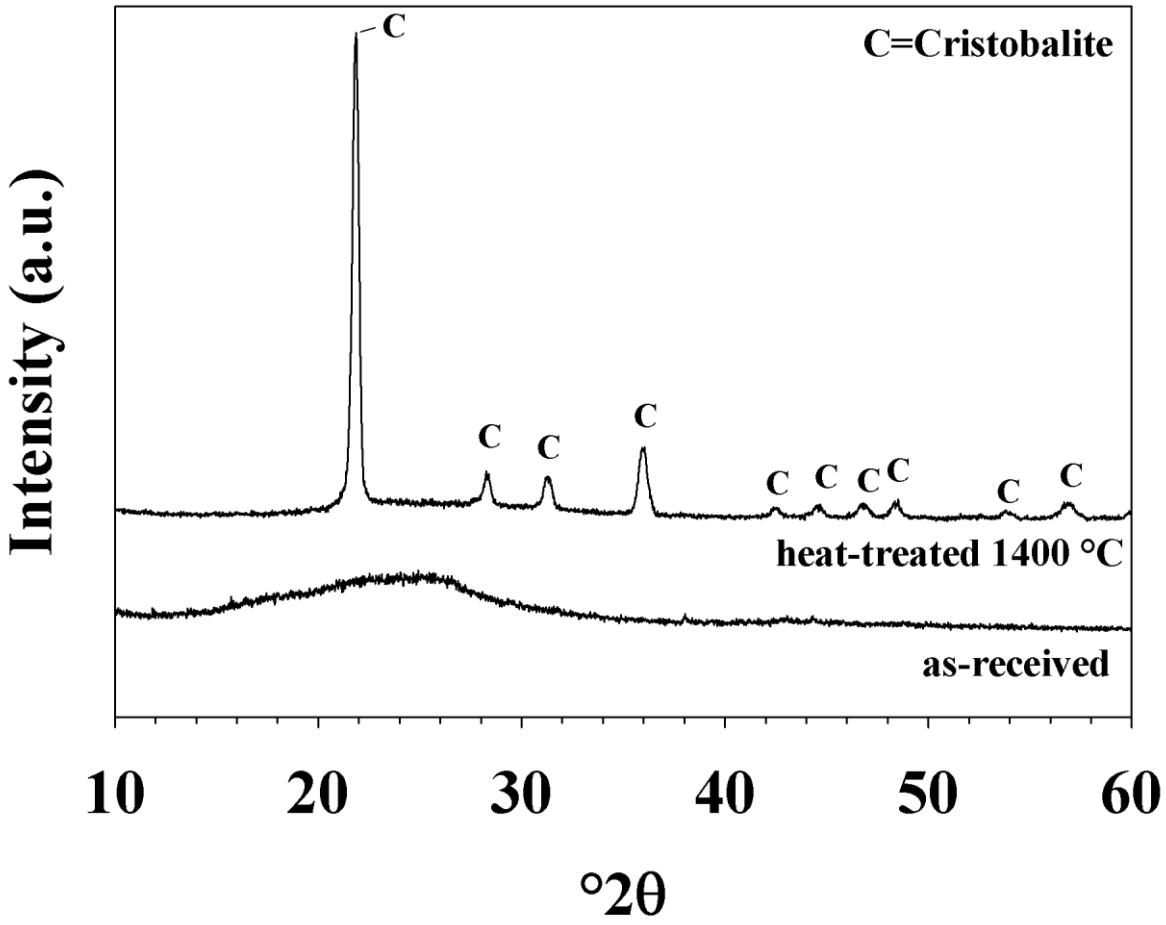

Fig. 11: FRAB-based insulation material during cone calorimetry testing.